Nature of Localized Excitons in $CsMgX_3$ (X = Cl, Br, I) and Their Interactions with Eu^{2+} Ions

Markus Suta,[1,†] Flavie Lavoie-Cardinal,[1,2,†] Jacob Olchowka,[1,3] and Claudia Wickleder[1,*]

[1]*Department of Inorganic Chemistry, University of Siegen, Adolf-Reichwein-Straße 2, 57068 Siegen, Germany*

[2]*L'Institut universitaire en santé mentale de Québec, 2601 Chemin de la Canardière, Québec QC G1J 2G3, Canada*

[3]*Département de Chimie Physique, Université de Genève, 30 Quai Ernest Ansermet, 1211 Genève, Switzerland*

(Received 14 June 2017; revised manuscript received 18 December 2017; published 15 June 2018)

In this paper, the luminescence properties of self-trapped excitons (STEs) of undoped and Eu^{2+}-doped perovskite-type materials $CsMgX_3$ (X = Cl, Br, I) are presented. The three compounds crystallize isostructurally in a hexagonal crystal system that exhibits an intrinsic pseudo-one-dimensionality. This feature has a highly stabilizing effect on the localization of excitons. The similarities to the properties of STEs in alkali halides are drawn that are justified by the band-structure and density-of-states calculations. The luminescence spectra of all three halides are characterized and interpreted despite their high complexity with many emissive transitions. It is illustrated that both STEs and impurity-localized self-trapped excitons (IL STEs) are responsible for the features in the spectra. The impurity localization of the STEs is proven by doping the hosts with Sr^{2+} ions instead of Eu^{2+} ions. The decay times in the microsecond range indicate that emission predominantly occurs from a triplet state of the STEs with a prominent afterglow component for the IL STEs that ideally suits a trapping model along the one-dimensional chains of the halides. Moreover, by thermal activation, the excitons tend to annihilate at the Eu^{2+} traps, thereby inducing an energy transfer to the Eu^{2+} ions. Because of this action, an extreme increase of the intensity of the Eu^{2+}-based $4f^65d$-$4f^7$ emission at room temperature is observed, which might be a general explanation for unusual temperature-dependent emission intensities of Eu^{2+} ions. In general, an understanding of the basic optical properties of the STEs may give some insights into the mechanism of currently used x-ray storage phosphors as well as scintillators.

DOI: 10.1103/PhysRevApplied.9.064024

I. INTRODUCTION

Many phosphors gain their luminescence properties by the intentional addition or even total composition of activators such as lanthanides, transition metals, or s^2 ions. Their applications range from light-emitting-diode phosphors over lasing materials to x-ray storage phosphors and scintillators [1]. Particularly for the last two applications, however, the optical properties of intrinsic defects that arise from the formation of excitons by incident ionizing radiation play a major role in the mechanistic details of the luminescence process [2,3]. Moreover, defects are generally created by doping if the size and/or the charge of the dopants and the substituted ion of the host do not coincide. In these cases, the defects influence the optical properties of the compounds usually remarkably due to quenching of the emissions of the activators or even due to intrinsic emission of defects stabilized by lattice distortions [2,3]. One prominent example is the x-ray storage phosphor $BaFBr:Eu^{2+}$ in which it was shown that point defects such as color centers are correlated with the local Eu^{2+} impurities, thereby influencing its photostimulable luminescence properties [4,5]. Therefore, defects and excitons are of key importance in the luminescence properties and the efficiency of materials and are, thus, worth investigating in detail.

In ionic insulators such as alkali halides, a created hole shows a high tendency for self-localization due to the high strength of the coupling to longitudinal optical phonons in these compounds that supports the formation of a polaronic quasiparticle [6–9]. Upon attraction of the electron, these self-trapped excitons (STEs) have a rich electronic structure that gives rise to complicated luminescence [10–15] and electron paramagnetic resonance (EPR) spectra [16–19]. The literature on the optical and magnetic properties of STEs in binary alkali halides is very exhaustive, and a very broad overview of the different properties is given in a review and a

*Corresponding author.
wickleder@chemie.uni-siegen.de

†These authors contributed equally to this work.

 © 2018 American Physical Society

book by Song and Williams in the 1990 s [20,21]. Since then, however, to the best of our knowledge, no comparably detailed literature on the optical properties of self-trapped excitons in more complex halides has been published so far.

In binary halides, it is now established that STEs can be well described by a "molecule-in-a-lattice" configuration in which the self-trapped hole forms a dimer anion X_2^- ($X = \mathrm{Cl}$, Br, I) and attracts the additional loosely bound electron without strong perturbation by the surrounding crystal field [16,22,23]. This ($V_k + e$) or on-center configuration is highly unstable against adiabatic relaxation in the lighter halides in which the electron first occupies an adjacent anion vacancy, thus, pushing the hole to the other anion vacancy [24–26]. A theoretical explanation for this phenomenon was first convincingly given by Toyozawa upon inclusion of a pseudo–Jahn-Teller mixing between the excited $|2p_z\rangle$- and $|1s\rangle$-like states of the electron [27]. From this off-center configuration, further separation of the electron and the hole gives rise to a separated *F*-*H* defect pair [25,26,28,29], which has also been proven experimentally [30]. Moreover, it has been shown in detailed investigations that this configuration is basically determined by the geometry of the crystal lattice that is parametrized according to Rabin and Klick [31] (see, also, Sec. III B of this paper and Refs. [28,32]).

In addition to binary alkali halides, there are only a few examples of more complex halides whose intrinsic luminescence were investigated, such as BaF*X* ($X = \mathrm{Cl}$, Br, I) [33–36], NH_4X ($X = \mathrm{Cl}$, Br, I) [37,38], or the fluoride-based perovskites $A\mathrm{MgF_3}$ ($A = \mathrm{K}$, Rb, Cs) [39–42].

One special class of halides that are interesting in this context are representatives of the $CsNiCl_3$ crystal structure such as $CsMnBr_3$ and $CsCdBr_3$ [43–45]. It is well known from these compounds that they show intrinsic luminescence ascribed to self-trapped excitons [46–53]. Compounds of this structure type exhibit an intrinsic pseudo-one-dimensionality due to linear chains of face-sharing coordination octahedra that allow a spontaneous self-trapping of excitons by electron-phonon coupling without a potential barrier [54]. This phenomenon is already well investigated in the related quasi-one-dimensional solids $[\mathrm{Pt(en)_2}][\mathrm{Pt(en)_2}X_2]Y_4$ with en = ethylenediamine ($C_2H_8N_2$), $X = \mathrm{Cl}$, Br, I, and Y as a complex anion such as ClO_4^- or PF_6^- in which the exciton forms as a result of an intervalence charge transfer and becomes self-trapped along a Peierls-distorted one-dimensional chain [21,55,56].

The one-dimensionality also allows for a movement of the excitation energy through the lattice along the linear chains, thus, also enabling energy-transfer processes [52,53]. Therefore, such systems are ideally suited for the investigation of the intrinsic electronic properties of STEs and their interaction with activators such as Eu^{2+}, which plays a tremendous role in the performance of novel scintillators or x-ray storage phosphors.

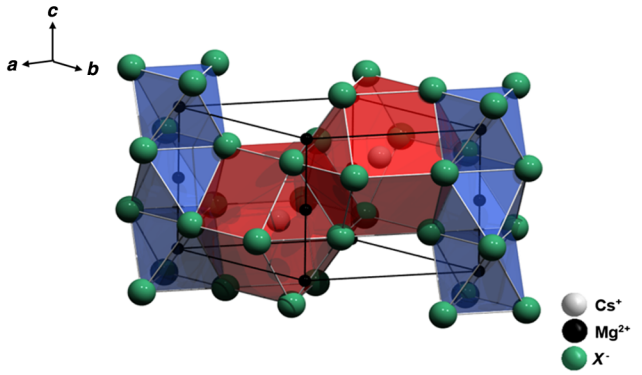

FIG. 1. Schematic view of the crystal structure of the quasi-one-dimensional halides $CsMgX_3$ ($X = \mathrm{Cl}$, Br, I). The Cs^+ ions are twelvefold coordinated, and the Mg^{2+} ions are sixfold coordinated by the X^- ions.

Based on the previous reasons, the intrinsic photoluminescence properties of STEs in the distorted perovskites $CsMgX_3$ ($X = \mathrm{Cl}$, Br, I) are presented in this paper, which also exhibit linear chains in their structure (see Fig. 1). In $CsMgCl_3$, an intrinsic luminescence has already been reported and also proven [57]. Moreover, this compound is known to show core-valence luminescence upon x-ray irradiation [58,59]. However, to the best of our knowledge, for $CsMgBr_3$ and $CsMgI_3$, no such studies have been reported yet. We, therefore, desire to present a systematic study of the varying optical properties of STEs as well as a comparison to binary alkali halides for these ternary compounds. Their chemical nature will be demonstrated with the aid of band-structure calculations. An efficient energy transfer to doped Eu^{2+} ions is illustrated, which makes these materials interesting for applications in the field of scintillators.

II. EXPERIMENT

A. Preparation

CsCl (Merck, 99.5%) and CsBr (Chempur, 99.9%) are predried at 200 °C in a dynamic vacuum overnight. The starting materials $MgCl_2 \times 6H_2O$ (Riedel-de Haën, 99%) and $MgBr_2 \times 6H_2O$ (Sigma Aldrich, 99%) are carefully dehydrated by sublimation under vacuum at 600 °C. All subsequent preparative steps are performed under dry Ar atmosphere in a glovebox (Braun).

$EuCl_2$ is synthesized in liquefied NH_3 using Eu metal (smart-elements, 99.99%) and vacuum-dried NH_4Cl (Th. Geyer, 99.8%) [60], whereas $EuBr_2$ and EuI_2 are directly obtained upon thermal decomposition under vacuum of the ternary halides $(NH_4)_3EuX_6$ ($X = \mathrm{Br}$, I) [61–64]. The ternary halides are synthesized from a solution of Eu_2O_3 (smart-elements, 99.99%) and the desired ammonium halide NH_4Br (Acros Organics, 99%) or NH_4I (Riedel-de Haën, 99%) in the half-concentrated acids HBr (Alfa Aesar) and HI (Merck), respectively, upon evaporation of the solvent.

The halides SrX_2 (X = Cl, Br, I) are also obtained upon drying of the respective hydrates $SrCl_2 \times 6H_2O$ (Riedel-de Haën, 99%), $SrBr_2 \times 6H_2O$ (Alfa Aesar, 99%), and $SrI_2 \times xH_2O$ (Heraeus, 99.5%) at 200 °C under vacuum. Strontium iodide is pretreated with diluted HI in order to remove traces of $SrCO_3$ that form upon standing in air.

The synthesis of the halides $CsSrX_3$ (X = Cl, Br, I) doped with 0.1 mol % Eu^{2+} is already described in the literature in detail [65–67]. For the preparation of the Eu^{2+}- and Sr^{2+}-codoped compounds $CsMgCl_3$ and $CsMgBr_3$, the corresponding anhydrous starting materials are fused together in stoichiometric amounts with small molar amounts of EuX_2 and/or SrX_2 (X = Cl, Br). Doped samples of $CsMgI_3$ are obtained by fusing CsI_3 (Alfa Aesar, 98%) with Mg metal (smart-elements, 99.8%) in stoichiometric amounts and doping the product with EuI_2 and/or SrI_2. All mixtures are sealed in evacuated silica ampoules, respectively, and melted at temperatures higher than the corresponding melting points according to the binary phase diagrams for 36 h [68–70]. Afterward, the mixtures are slowly (2 °C/h) cooled to 100 °C below the melting point and finally to room temperature at a rate of 10 °C/h. The purity of all samples is verified by x-ray powder diffraction (Stoe Stadi P, Cu K_α radiation; see Ref. [71]).

B. Optical measurements

Clear and transparent pieces (approximately 1 mm^3) of the products are sealed in evacuated thin silica ampoules for photoluminescence investigations. The emission and excitation spectra are detected with a Fluorolog-3 (FL3-22) spectrofluorometer (Horiba Jobin Yvon) equipped with a 450-W Xe lamp and double Czerny-Turner monochromators that allow a resolution down to 0.05 nm. The signal is detected with a photomultiplier tube R928P (Hamamatsu) coupled with a photon-counting system. The emission spectra are corrected for the photomultiplier sensitivity and excitation spectra for the lamp intensity. A He closed-cycle cryostat (Janis) allows measurements between 10 K and room temperature. Decay times down to 5 μs are measured at 10 K using a 75-W Xe flash lamp that is attached to the same spectrometer. The diffuse reflectance measurements are performed with a Cary 5000 UV-vis spectrometer (Agilent) that detects reflectance between 200 and 2500 nm. The reflectance spectra are corrected for the background with a Spectralon reference sample.

C. Band-structure and density-of-states calculations

The calculations of the band structures and the density of states (DOS) of the host compounds are performed with the Vienna *ab initio* simulation package [72–76]. All calculations are carried out within the generalized-gradient approximation (GGA) by a Perdew-Wang functional (PW91) to account for the exchange and correlation functionals [77–79]. The interaction between the core and valence electrons is approximated in terms of the projected-augmented-wave method [80,81]. Full geometry optimizations are performed with a cutoff energy of 550 eV and 10 k points in the Brillouin zone. The atomic positions are allowed to relax until the residual Hellmann-Feynman forces are smaller than 0.03 eV/Å. The band-structure and density-of-states calculations are conducted with the relaxed structures and a plane-wave cutoff energy of 400 eV and 20 k points in each direction. Convergence is achieved for energy variations smaller than 10^{-6} eV.

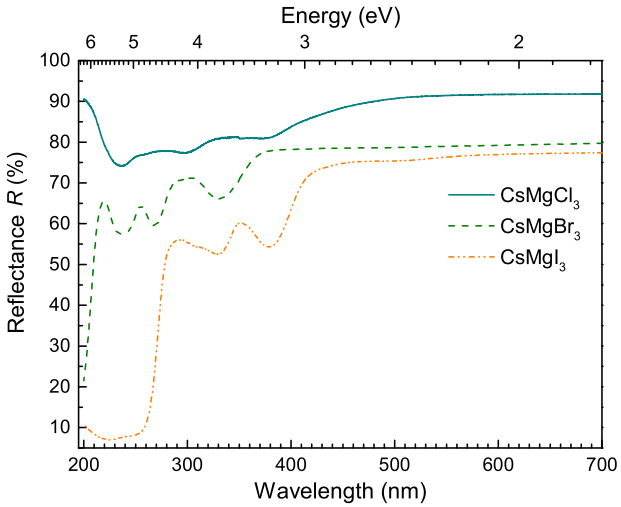

FIG. 2. Diffuse reflectance spectra of the undoped halides $CsMgCl_3$, $CsMgBr_3$, and $CsMgI_3$ at room temperature.

III. RESULTS AND DISCUSSION

A. Band-structure and electronic DOS calculations

Figure 2 depicts the reflectance spectra of the undoped halides $CsMgCl_3$, $CsMgBr_3$, and $CsMgI_3$. In the cases of $CsMgBr_3$ and $CsMgI_3$, strong absorption bands are detected at high energies, which are readily recognized as transition from the valence to the conduction band and allow a determination of the optical band gaps as given in Table I. In particular, our experimentally determined value for the band gap of $CsMgI_3$ (4.57 eV) is in very good agreement with an earlier measurement by McPherson and Talluto (4.84 eV) [82]. In the case of $CsMgCl_3$, the band-band transition is energetically above the measurable range of the reflectance spectrometer. Additionally, several small absorption bands are present at energies lower than the

TABLE I. Calculated and experimental band gaps of $CsMgX_3$ (X = Cl, Br, I). For details on the calculations, see text.

Compound	E_g (theoretical) (eV)	E_g (experimental) (eV)
$CsMgCl_3$	5.24	>6(8.50)[a]
$CsMgBr_3$	4.16	5.95
$CsMgI_3$	3.13	4.57

[a]References [58,59].

TABLE II. Characteristic values of optical properties of the STEs in $CsMgX_3$ (X = Cl, Br, I). All measured values are acquired at 10 K. For details, see text.

Compound	Rabin-Klick parameter S/D	E_{em} (cm^{-1})	FWHM (cm^{-1})	Stokes shift ΔS (cm^{-1})	τ (μs)
$CsMgCl_3$	0.1624	25 700 (π)	2110 (π)	11 860 (π)	35 (π)
$CsMgBr_3$	0.1038	24 610 (π)	2470 (π)	11 600 (π)	57 (π)
		29 410 (σ)	2240 (σ)	2680 (σ)	<10 (σ)
$CsMgI_3$	0.0286	25 520 (π)	3240 (π)	13 660 (π)	11 (π)

actual band-band transition, which can, therefore, be assigned to transitions into the different excitonic hydrogenlike states $|n\rangle$. Since all of the compounds crystallize in the same hexagonal crystal system with space group $P6_3/mmc$ (no. 194) [45,83], the band structures and DOS look accordingly similar (see Fig. 2). All halides show a direct band gap at both the Γ and K point, which decreases for the heavier halides, in agreement to expectations. Moreover, the calculated value of 5.24 eV for $CsMgCl_3$ agrees well with the recently reported value of 5.31 eV [84]. However, the theoretical values are lower than the experimentally determined band gaps (see Fig. 2 and Table II). This is a well-known fact from GGA DFT calculations due to the approximation in the electron exchange-correlation functional [85,86] and the energy derivative discontinuities that arise from the integer number of electrons [87,88].

The low curvature of the valence band close to the Γ point in all three compounds indicates a high effective hole mass, whereas the effective electron mass is much lower according to the curvature of the lowest conduction band. This confirms the formation of STEs in the manner that is known from the binary alkali halides [16]. In particular, the direct band gap of all three compounds $CsMgX_3$ (X = Cl, Br, I) also suggests that the formation of excitons should be very efficient.

In general, several main groups of bands can be distinguished in all three compounds according to the DOS calculations (see Fig. 3). The narrow core bands between −15 and −10 eV have dominant s orbital contribution from the halide anions with very small mixing of the Mg $2s$ and $2p$ character in all compounds. Additionally, at around −8 to −6 eV, dominant $5p$ core bands from the Cs atoms are present in all cases, which shift to lower energies and become narrower for the heavier halides. This behavior is reasonable since valence orbitals of the halides increase in energy with higher atomic number and lower electronegativity and, therefore, make the Cs core bands more nonbonding and, hence, dispersionless. Since the gap between the upper edge of the valence bands and the core band E_{VC} increases for the heavier halides, only $CsMgCl_3$ is expected to show core-valence luminescence ($E_{VC} < E_g$), which agrees with reported observations [58,59].

The calculations additionally show that the lowest valence bands are most dominantly composed of Mg $2s$ orbitals. For the uppermost valence bands, the p orbitals of the halide anions show by far the highest contribution, whereas also slight mixing of the Mg $2p$ and Cs $5p$ orbitals is obvious. Just below the Fermi level, however, only p bands from the halides are present. The lowest conduction bands are mainly composed of Mg $3s$ orbitals. At higher energies (5–10 eV), conduction bands with mainly $5d$ contribution of the Cs ions and little mixing of Mg $2p$ orbitals as well as halogen s, p, and d orbitals (for Br and I) are present (note the scales in Fig. 3).

The projected DOS calculations especially indicate a striking similarity of the electronic properties of the compounds $CsMgX_3$ (X = Cl, Br, I) to the simple binary alkali halides [21], which is mainly related to the high ionicity in this compound. In fact, the sole contribution of the halogen p orbitals at the Fermi level and the Mg $3s$ orbitals at the bottom of the conduction bands confirms the previously stated argument that STEs in the presented compounds form in a similar way as known for the alkali halides. Moreover, the strong participation of Mg on the lowest conduction band allows us to conclude that the STEs are strongly confined along the linear chain of face-sharing $[MgX_6]^{4-}$ octahedra in the direction of the hexagonal c axis. This is in agreement to the reported luminescence properties of STEs in isostructural compounds such as $CsMnBr_3$ or $CsCdBr_3$ [47,51–53]. Because of the intrinsic one-dimensionality that is also exhibited in the compounds $CsMgX_3$ (X = Cl, Br, I), STE formation should be highly favored [54].

B. Photoluminescence of self-trapped excitons in $CsMgX_3$ (X = Cl, Br, I)

Figure 4 shows that STEs are detectable in the UV range and are intrinsic to the hosts $CsMgCl_3$, $CsMgBr_3$, and $CsMgI_3$. Because of the dense packing of the perovskite-based structures of $CsMgCl_3$, $CsMgBr_3$, and $CsMgI_3$, STEs should predominantly orient along the hexagonal c axis at 10 K, as already suggested for $CsMnBr_3$ and $(CH_3)_4NMnX_3$ (X = Cl, Br) [89,90]. The corresponding Rabin-Klick parameters for an orientation along the [011] direction are $S/D = 0.1624$, 0.1038, and 0.0286 for $CsMgCl_3$, $CsMgBr_3$, and $CsMgI_3$, respectively. Here, S denotes the distance between two adjacent halide anions in the regarded direction minus the halide ionic diameter, whereas D is the diameter of the corresponding free halogen atom [28,31,32]. S/D is a measure for the tendency to separate the self-trapped hole from the electron,

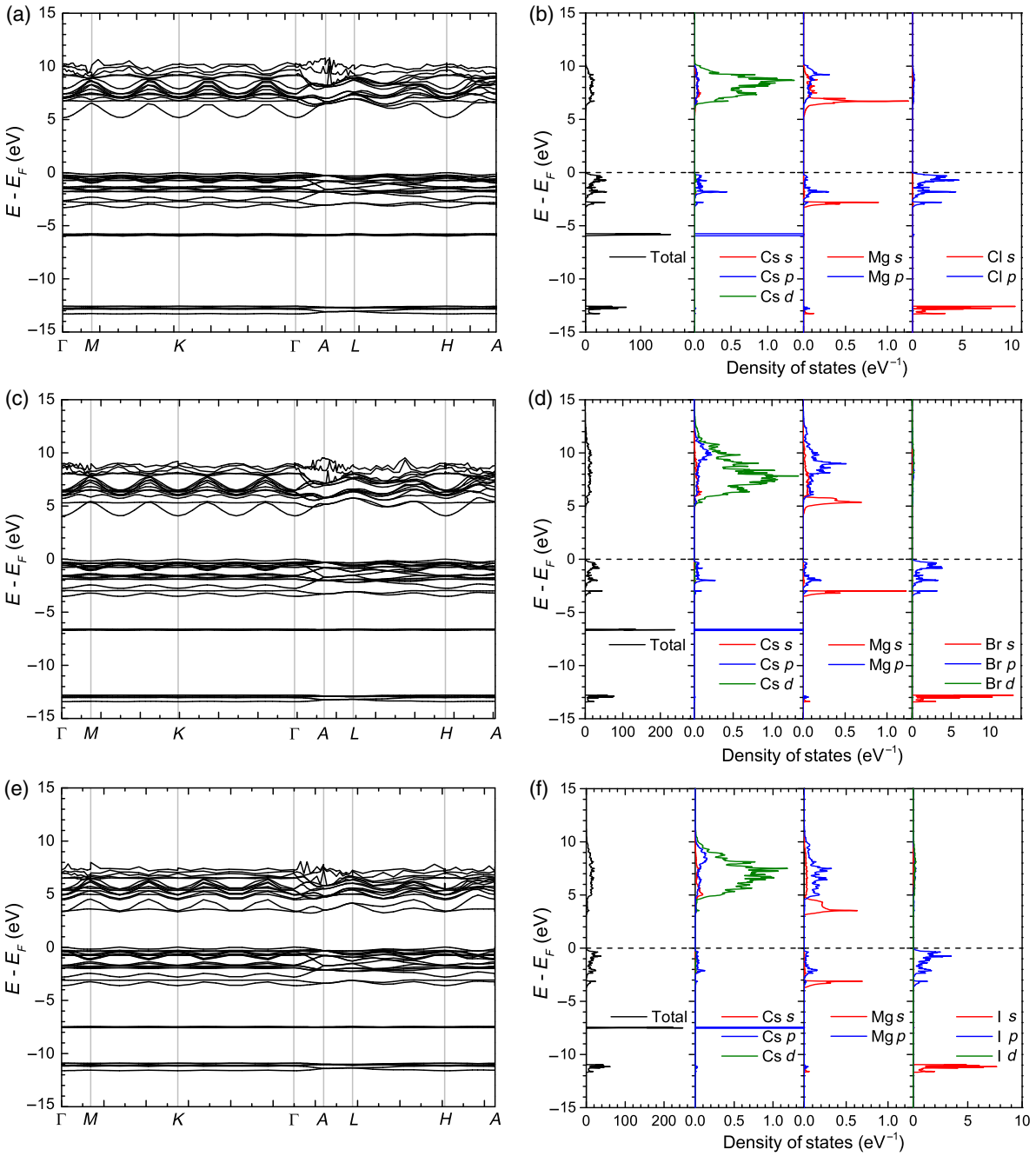

FIG. 3. Calculated band structures and electronic total as well as projected DOS of $CsMgCl_3$ (a),(b), $CsMgBr_3$ (c),(d), and $CsMgI_3$ (e),(f).

thereby forming an F-H defect pair, in which both electron and hole occupy a single anion vacancy, respectively. The low values of S/D for the presented compounds compared to alkali halides indicate that the STEs in $CsMgX_3$ (X = Cl, Br, I) and accordingly in similar quasi-one-dimensional compounds tend to be on centered and can, hence, be well described within the $(V_k + e)$ or type I configuration according to the classification of Kan'no *et al.* [28,29].

The low Rabin-Klick parameters imply that a singlet or σ emission should also be observed, which is characterized by low Stokes shifts [20,21]. In fact, a UV emission band is observed at 340 nm (29 410 cm^{-1}) in $CsMgBr_3$ [see Fig. 4(b)] with a Stokes shift of 2680 cm^{-1}. Another lower energetic emission at 406 nm (24 610 cm^{-1}) is correspondingly assigned to a triplet or π emission. The respective excitation spectra are characterized by broad featureless bands in proximity to the conduction band, which additionally justifies the assignment.

For the other two halides, only one emission can be observed with similarly broad and featureless excitation bands [see Figs. 4(a) and 4(c)]. In $CsMgCl_3$, it is located at 25 700 cm^{-1} (389 nm), whereas in $CsMgI_3$, the emission is

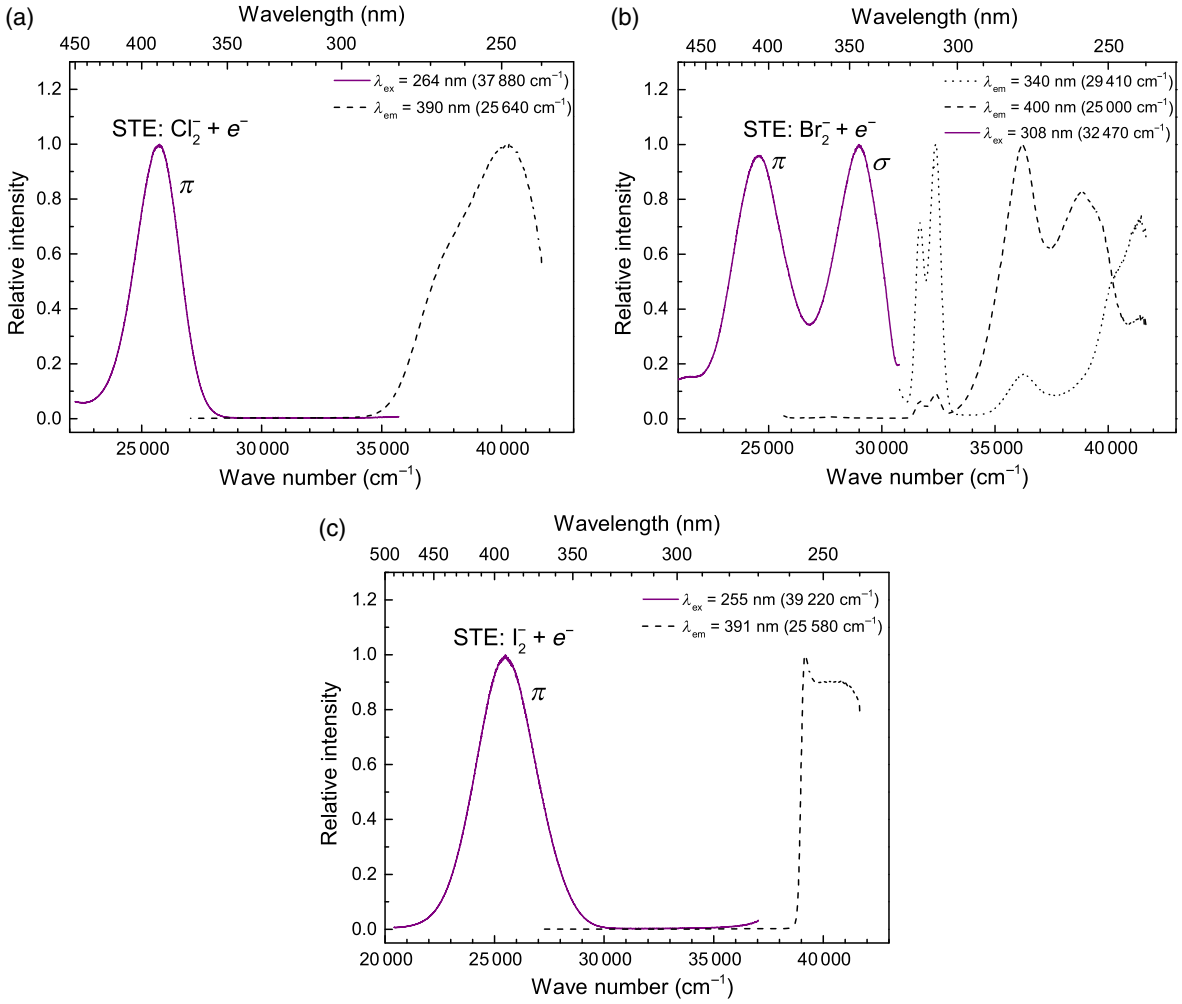

FIG. 4. Photoluminescence emission (solid) and excitation spectra (dashed or dotted) of STEs in undoped (a) $CsMgCl_3$, (b) $CsMgBr_3$, and (c) $CsMgI_3$ at 10 K. The π and σ emissions are indicated in each case.

peaking at 25 520 cm^{-1} (392 nm) in perfect agreement with the reported value for the intrinsic emission in this iodide [82]. According to the decay times (see Sec. III C), they are also assigned to π transitions. All three π emissions are characterized by very large Stokes shifts (11 860, 11 600, and 13 660 cm^{-1} for $CsMgCl_3$, $CsMgBr_3$, and $CsMgI_3$, respectively) similar to the alkali halides [20,21], which additionally justifies the assignment. Interestingly, the positions of all three π emission bands are very similar to each other. This may be assigned to a compensating effect between the expected redshift due to the higher degree of polarizability of the heavier halides and the stronger constraint of the surrounding lattice in formation of the STEs as indicated by the Rabin-Klick parameters S/D.

C. Decay times of self-trapped excitons in $CsMgX_3$ (X = Cl, Br, I)

The decay curves obtained upon detection of the emissions from the STEs and impurity-trapped excitons (ITEs) in $CsMgCl_3$, $CsMgBr_3$, and $CsMgI_3$ show a multiexponential behavior with decay times in the microsecond range and an afterglow component in the range of tens of milliseconds at 10 K (see Ref. [71]). These decay times clearly identify the transitions as tripletlike or π emissions in analogy to alkali halides [15,20,21]. Only the shortest components are interpreted due to the arbitrariness of the multiexponential fitting function in order to crudely model the afterglow. In general, the decay time of the π emissions decreases with heavier halide due to the increasing impact of spin-orbit coupling that mixes singlet character into the excited state of the STE, hence, allowing the π emission at all. The decay time of the triplet state $^3\Sigma_u^+$ is given by [15,29].

$$\tau_\pi^{-1} = CE_\pi^3 b^2 |\langle {}^1\Pi_u | \vec{r} | {}^1\Sigma_g^+ \rangle|^2, \quad (1)$$

where C is a constant, E_π is the π emission energy, and b is the mixing coefficient indicating the amount of singlet-triplet mixing that is proportional to the spin-orbit-coupling constant ζ of the free halogen atom. The radial integral accounts for the transition dipole moment between the excited and ground singlet state of the STE. Since the emission energies

for the STEs do not vary significantly in the regarded isostructural compounds $CsMgX_3$ (X = Cl, Br, I), the main impact on the decay time arises from the mixing parameter b and, hence, the spin-orbit coupling and the exchange splitting ΔE_{ex} between the singlet and triplet state. In the weak perturbation limit, it is [15,29]

$$b = \frac{\zeta}{\Delta E_{ex}}. \quad (2)$$

In the case of the presented halides, the shortest decay time components are assigned to the π emission and read 35 μs in $CsMgCl_3$, 57 μs in $CsMgBr_3$, and 11 μs in $CsMgI_3$ at 10 K. Since the spin-orbit-coupling constant ζ increases from the chloride to the iodide, the initial increase in decay time from the chloride to the bromide may be related to a compensating effect from the decrease in the π emission energy. The relatively low decay times in the microsecond range compared to the values from some alkali halides in the millisecond range [15,20,21,28,29] are ascribed to the difference in Rabin-Klick parameters S/D and the corresponding amount of relaxation of the STEs. In $CsMgX_3$, the S/D values are comparably low, thereby leading to type I STEs with considerable singlet character of the excited states. In alkali halides, the more open structure allows for a higher degree of structural relaxation of the STEs also reflected in the larger S/D values [21]. These structural features typically lead to the sole observation of a π emission and, therefore, larger decay times due to the larger triplet character.

A corresponding decay time for the singlet or σ emission is below the detectable limit of the employed flash lamp (<10 μs), thereby justifying the assignment. Unfortunately, a corresponding measurement with a pulsed laser is not possible at the necessary cryogenic temperature.

D. Photoluminescence spectra of impurity-localized excitons in $CsMgX_3:Eu^{2+}$

The $4f^6 5d \rightarrow 4f^7$ luminescence of Eu^{2+} located at the Mg^{2+} sites in $CsMgX_3$ (X = Cl, Br, I) has already been discussed in detail in the literature [66,67,91]. Only one redshifted emission band due to the $4f^6 5d \rightarrow 4f^7$ transition of Eu^{2+} ions is observed in each case. The occupation of the small Mg^{2+} sites has so far been proven by structure-luminescence relationships and theoretical considerations [66,67,92]. However, a second dominant emission is visible in the blue range in each of the halides (see Fig. 5). Their maxima are located at 23 360 cm^{-1} (428 nm), 22 990 cm^{-1} (435 nm), and 22 320 cm^{-1} (448 nm) for $CsMgCl_3$, $CsMgBr_3$, and $CsMgI_3$, respectively. Additionally, redshifted emission bands peaking at 21 740 cm^{-1} (460 nm) in $CsMgCl_3$ and 21 050 cm^{-1} (475 nm) in $CsMgBr_3$ are detected upon excitation with UV light [see Figs. 6(a) and 6(c), upper spectra]. The presence of these bands is not trivially understood since the crystal structure of the presented halides intuitively allows only one additional emission band in addition to the one due to Eu^{2+} located on the Mg^{2+} sites that can formally be assigned to another $5d-4f$ emission of Eu^{2+} on the respective twelvefold-coordinated Cs^+ sites. Also, the energetic positions of the blue emission bands are reasonable for that assumption if compared to the emission energies of Eu^{2+} in CsCl (E_{em} = 22 730 cm^{-1}), CsBr (E_{em} = 22 680 cm^{-1}), and CsI (E_{em} = 22 370 cm^{-1}) [93–95]. However, the mismatch both in charge and the Shannon ionic radii of Cs^+ [$r(Cs^+)$ = 1.88 Å] and Eu^{2+} [$r(Eu^{2+})$ = 1.43 Å] might imply that this situation is not highly probable [96]. Moreover, as we indicate above, the preliminary studies already excluded this interpretation for low concentrations (<3 mol %) [66,67,92].

In order to elucidate the nature of the blue luminescence in the Eu^{2+}-doped halides $CsMgX_3$, a concentration series with Eu^{2+} and Sr^{2+} is investigated (see Fig. 5). With increasing Sr^{2+} concentration, the Eu^{2+}-based $4f^6 5d \rightarrow 4f^7$ emission band decreases in intensity in agreement with expectation, whereas the blue emission band retains its intensity. This indicates that the distortion caused by the ionic mismatch between Eu^{2+} or Sr^{2+}, respectively, and Mg^{2+} is crucial for the origin of the blue luminescence bands [96].

The appearance of the photoluminescence excitation spectra (cf. Fig. 6) upon detection of the corresponding blue emission bands additionally show a striking similarity to the excitation spectra from $CsSrX_3:Eu^{2+}$ (X = Cl, Br, I) both in energies and fine structure (see Fig. 6, lower panels). The position of the higher-energetic blue emission band agrees very well with the emission bands of Eu^{2+} in the previously mentioned Sr-based halides [66,67]. Thus, the intense emission bands peaking at 23 360 cm^{-1} (428 nm), 22 990 cm^{-1} (435 nm), and 22 320 cm^{-1} (448 nm) for $CsMgCl_3$, $CsMgBr_3$, and $CsMgI_3$, respectively, are assigned to impurity-localized STEs (IL STEs) at the Eu^{2+} ions. It should be noted at this stage that this term is not to be confused with the also currently prominent ITEs in, e.g., Yb^{2+}-doped fluorides that contrarily stem from photoionization of the Yb^{2+} ions upon excitation of the electron into the conduction band [97–104]. The IL STEs regarded in this paper refer to mobile polaronic STEs along the linear chains in $CsMgX_3$ (X = Cl, Br, I), which become occasionally localized at impurities.

A reasonable explanation for the assignment to IL STEs is possible upon referring to the works on excitons in compounds with face-sharing octahedra such as CdX_2 (X = Cl, Br, I) or especially $CsCdBr_3$ [49,105,106]. Upon doping the halides $CsMgX_3$ (X = Cl, Br, I) with Eu^{2+}, their $5d$ orbitals are located in the band gap and can, therefore, interact with the np orbitals of the halide anions to form covalent bonds. Accordingly, the localized excitons in close proximity to the Eu^{2+} sites may be described in terms of a whole $[EuX_6]^{4-}$ octahedron (X = Cl, Br, I) within the linear chains along the hexagonal c axis instead of simple perturbed STEs. The similarity of the excitation spectra of the ITEs to the excitation spectra of isolated Eu^{2+}

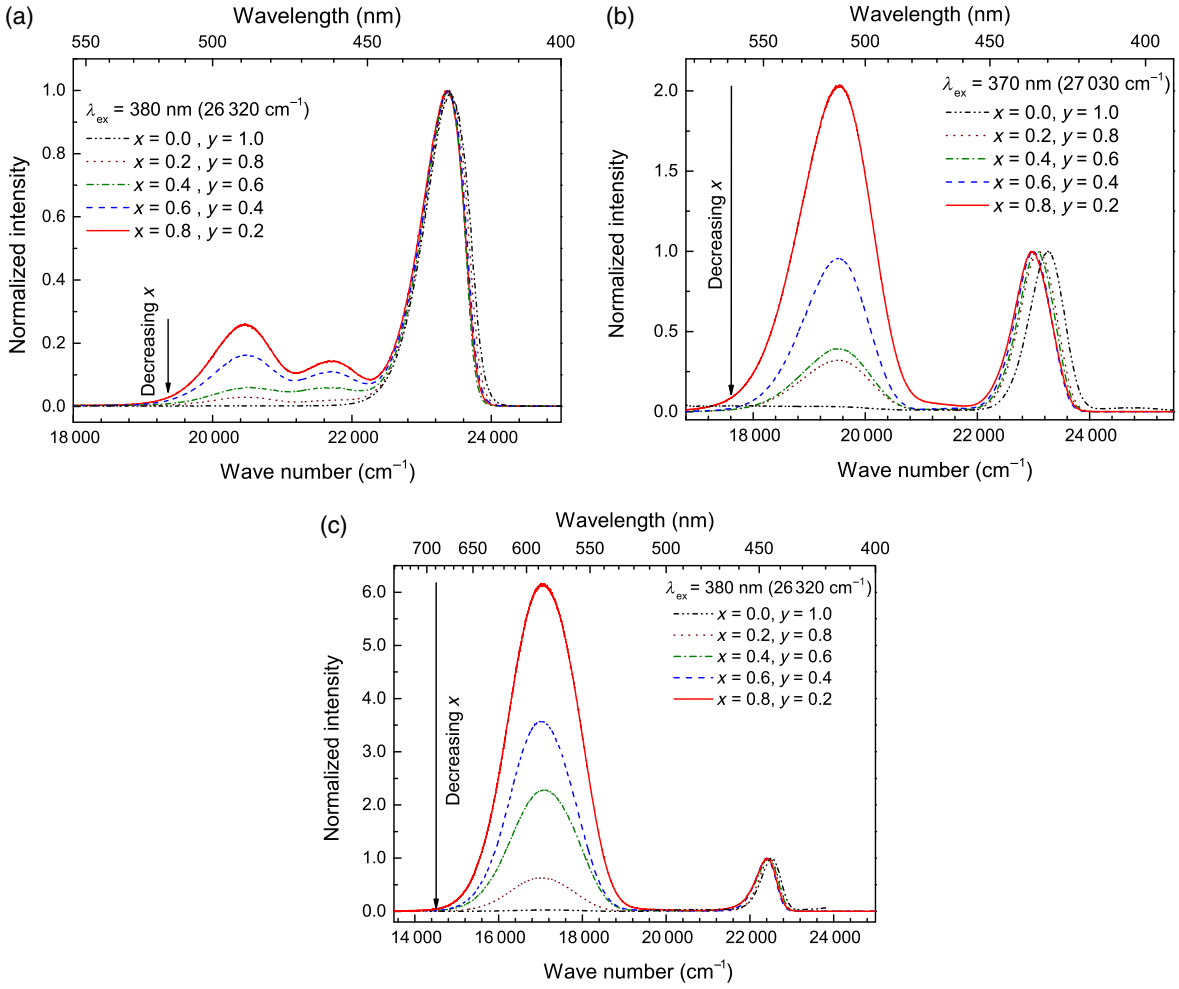

FIG. 5. Emission spectra at 10 K of (a) $CsMgCl_3$: $x\%$ Eu^{2+}, $y\%$ Sr^{2+}, (b) $CsMgBr_3$: $x\%$ Eu^{2+}, $y\%$ Sr^{2+}, and (c) $CsMgI_3$: $x\%$ Eu^{2+}, $y\%$ Sr^{2+}. The total doping concentration is always $(x+y)\% = 1\%$.

centers in $CsSrX_3$ [65–67] is a strong hint on this idea and arises from the fact that Eu^{2+} and Sr^{2+} have nearly similar ionic radii $[r(Eu^{2+}) = 1.17$ Å, $r(Sr^{2+}) = 1.18$ Å] and, therefore, characterize perfectly isolated $[EuX_6]^{4-}$ octahedra [96]. Therefore, the actual excited states of the IL STEs are strongly localized on the Eu^{2+} ions, which may be interpreted in a decoupled scheme that treats the $4f^6$ core separately from the $5d$ orbital and has been discussed in detail by us earlier [66,67]. The observation that two blue emissions are observed in Eu^{2+}-activated $CsMgCl_3$ and $CsMgBr_3$ is explained by a perturbation from the local crystal field due to the ionic mismatch between the Eu^{2+} and Mg^{2+} ions. In the iodide, the metal-ligand distances are, however, longer such that the local perturbation is assumed to be negligibly weak.

Alternatively, the incorporation of Eu^{2+} ions might also lead to stacking faults in the sense that the $[EuBr_6]^{4-}$ are tilted instead of face sharing in the original structure of $CsMgX_3$. Calculations or EPR measurements, which give further insight into the local structure of the IL STEs, are planned.

E. Analysis of the afterglow of the luminescence of impurity-localized excitons

In the photoluminescence decay curves of the IL STEs, an additional afterglow component in the decay curve becomes more dominant (see Fig. 7, lower panels), thus, excluding a pure $4f^65d \rightarrow 4f^7$ emission of interstitial Eu^{2+} ions and justifying the attempted assignment. Contrarily, the decay times of the proposed $4f^65d \rightarrow 4f^7$ emission of Eu^{2+} at the Mg^{2+} sites are below 1 μs at room temperature and do not increase above 10 μs even at 10 K [66,67]. The shortest components of the decay curves characteristic of the IL STEs are very similar to the decay times obtained for the STEs (see Table II), which indicates that they indeed are formed by localization of the excitons at the Eu^{2+} impurities. It is shown that trapping of excitons at local impurities in an ideal one-dimensional chain should follow a $t^{-0.5}$ dependence in the decay curve, which was also

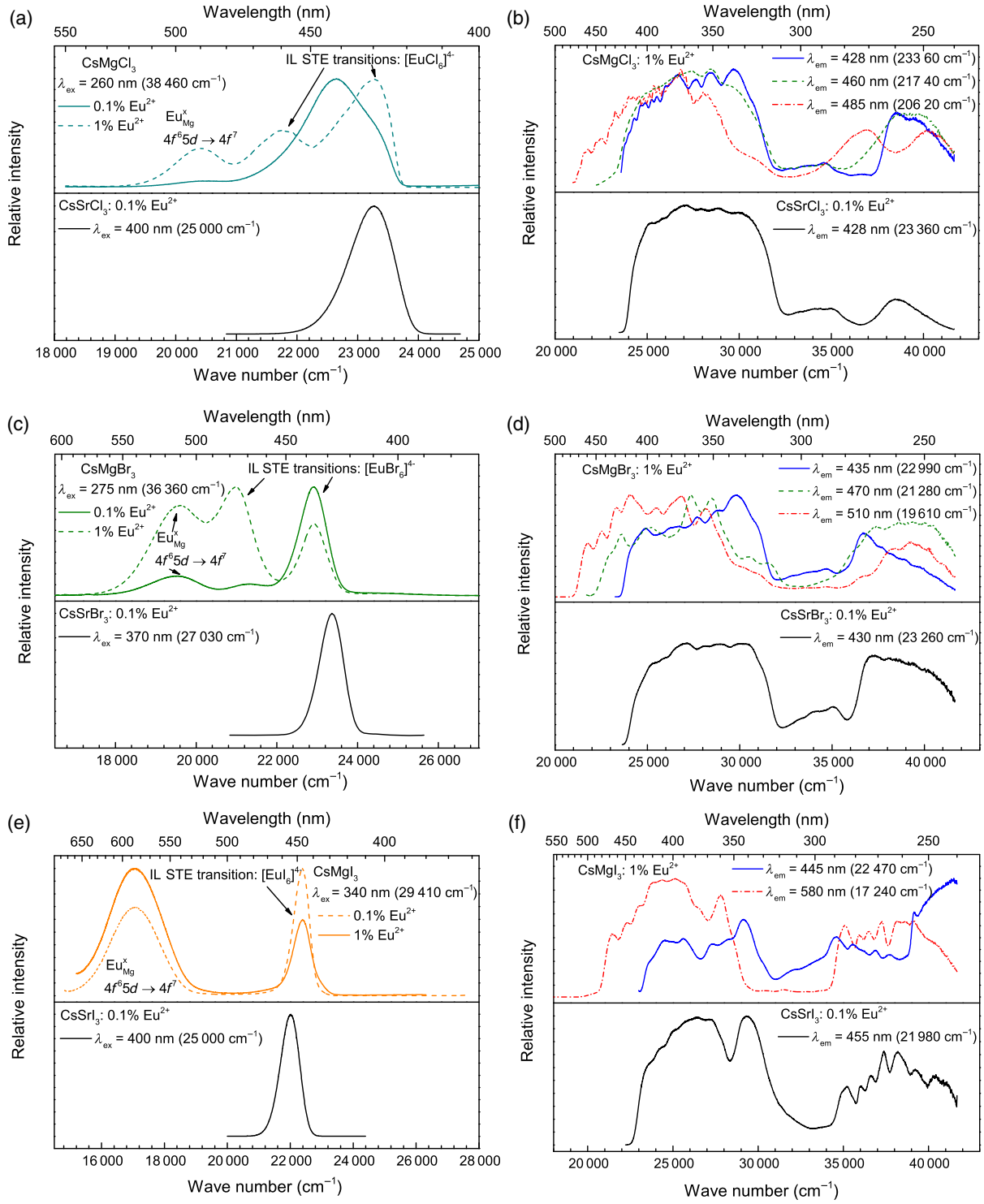

FIG. 6. Photoluminescence emission spectra recorded at 10 K for (a) $CsMgCl_3:Eu^{2+}$, (c) $CsMgBr_3:Eu^{2+}$, and (e) $CsMgI_3:Eu^{2+}$. Solid lines denote a doping concentration of 0.1 mol %, and dashed lines are a doping concentration of 1-mol % Eu^{2+}. The assignments of the emissions arising from $4f^65d \rightarrow 4f^7$ emissions of Eu^{2+} on Mg^{2+} sites are indicated. The lower spectra depict the $4f^65d \rightarrow 4f^7$ emissions of Eu^{2+} in $CsSrX_3$ (X = Cl, Br, I), respectively (cf., also, Refs. [65–67]). The corresponding photoluminescence excitation spectra upon detection of the IL STE transitions are also given for (b) $CsMgCl_3:1\%\,Eu^{2+}$, (d) $CsMgBr_3:1\%\,Eu^{2+}$, and (f) $CsMgI_3:1\%\,Eu^{2+}$ at 10 K. The dashed curves relate to the $4f^65d \rightarrow 4f^7$ emission of Eu^{2+} on the Mg^{2+} sites. The corresponding excitation spectra.

experimentally confirmed [90,107]. The afterglow components of the decay curves related to the IL STEs in $CsMgX_3:0.1\%\,Eu^{2+}$ (X = Cl, Br, I) can be well fitted to a $t^{-0.4}$ to $t^{-0.7}$ decay instead. The deviation from the ideal case is interpreted to arise due to the possibility of interchain diffusion as the Cs^+ ions are not bulky enough to confine the exciton formation exclusively to the linear chains in the structure [90]. The decay kinetics, therefore, also justifies the picture of exciton trapping at the present Eu^{2+} impurities.

F. Thermal annihilation of excitons at Eu^{2+} ions in $CsMgX_3$ (X = Cl, Br, I)

Both the π emissions of the STEs as well as the most intense IL STE transition in all three halides (see Figs. 4 and 6) overlap with the excitation bands of Eu^{2+}, thus, fulfilling the resonance condition of an energy transfer from excitons to Eu^{2+}. Since the decay times of the excitonic transitions (see Table II and Fig. 7) do not vary significantly with varying Eu^{2+} concentration within the range of 0.1–1 mol %, a classical resonance-type energy transfer according to Förster [108] or Dexter [109] may be excluded. Upon excitation in the UV range, the intensity of the Eu^{2+}-based luminescence in the samples $CsMgI_3:1\%\,Eu^{2+}$ increases with increasing temperatures (see Fig. 8). This is especially pronounced for $CsMgBr_3:1\%\,Eu^{2+}$, where the highest intensity of the Eu^{2+} emission is detected at room temperature. An increasing luminescence intensity with increasing temperature is an unusual observation if classical thermal quenching upon coupling to local vibrational modes is taken into account, and so far, only rarely reported [110]. Here, a thermally assisted energy transfer to the Eu^{2+} ions by the localized excitons must be indicated, most probably by thermal annihilation. A possible energy-transfer mechanism that was thoroughly investigated in the class of quasi-one-dimensional compounds relies on the possibility of exciton hopping within the linear chains along the hexagonal c axis [52,53]. The hopping diffusion of the excitons is based on a

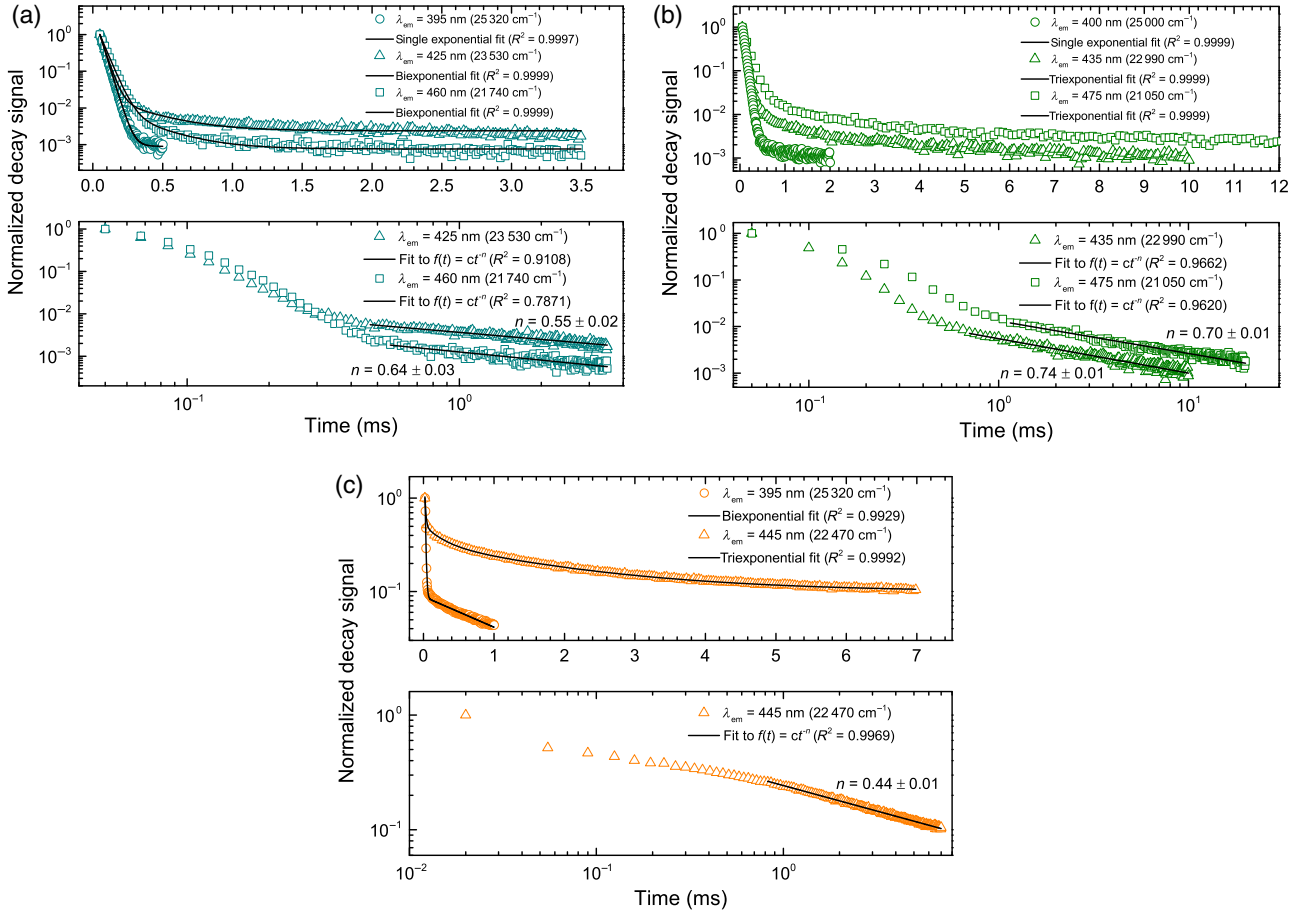

FIG. 7. Upper panels: Photoluminescence decay curves of (a) $CsMgCl_3:0.1\%\,Eu^{2+}$ (λ_{ex} = 248 nm), (b) $CsMgBr_3:0.1\%\,Eu^{2+}$ (λ_{ex} = 275 nm), and (c) $CsMgI_3:0.1\%\,Eu^{2+}$ (λ_{ex} = 255 nm) for the π emissions of the STEs as well as the emissions of the IL STEs. Lower panels: Double-logarithmic plots of the decay curves of the IL STE transitions indicating the t^{-n} dependence of the afterglow components. Fitting curves are indicated as solid lines.

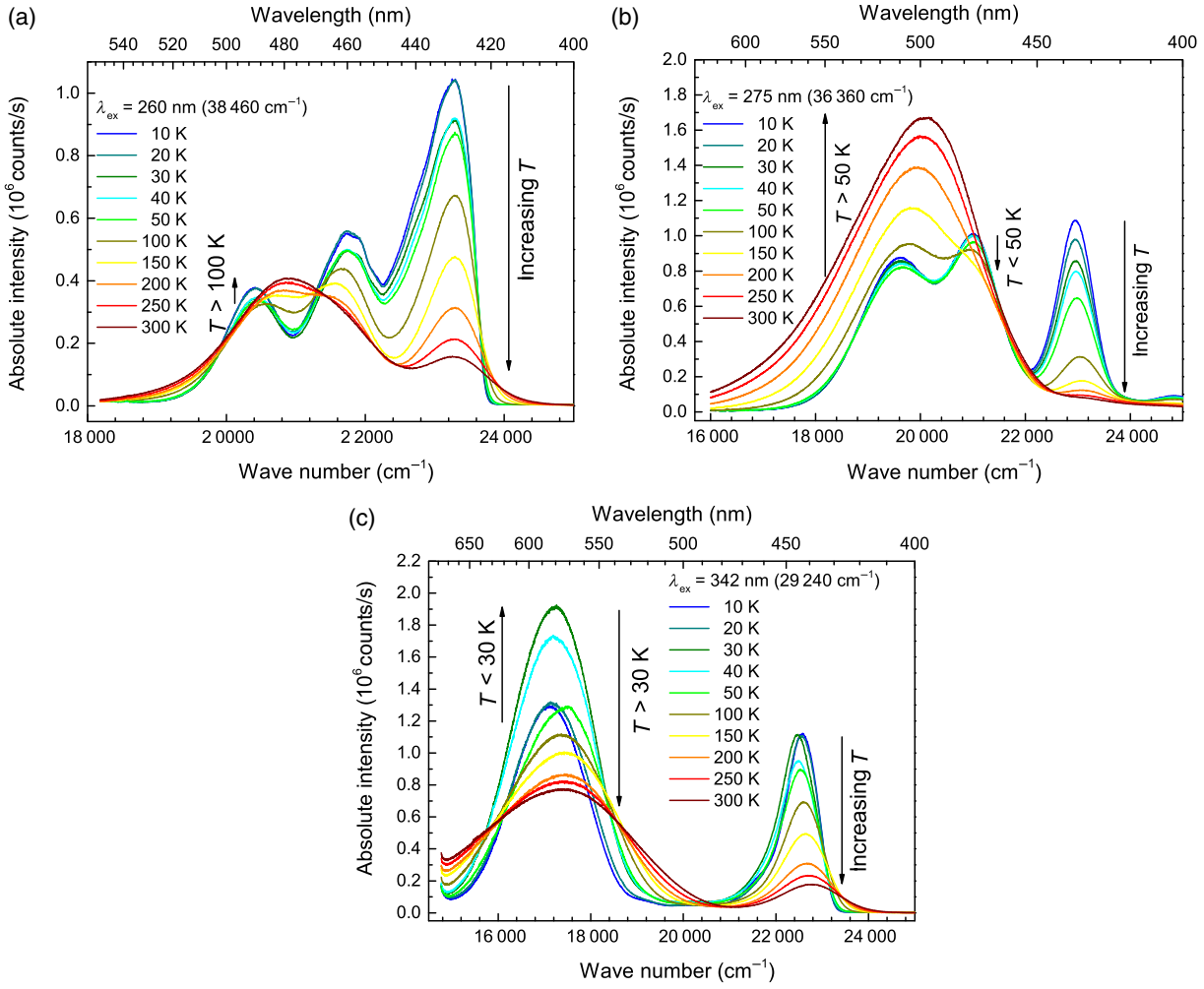

FIG. 8. Temperature-dependent emission spectra of (a) $CsMgCl_3:1\%\,Eu^{2+}$, (b) $CsMgBr_3:1\%\,Eu^{2+}$, and (c) $CsMgI_3:1\%\,Eu^{2+}$. In all three cases, a UV excitation wavelength is used for the purpose of an efficient excitation into STE states.

"zigzaglike" movement, in which the bonds of the V_k center X_2^- fold along the c axis. Hence, the activation energy for the hopping mechanism should correlate with the binding energy of the V_k center X_2^- ($X = \mathrm{Cl}$, Br, I) [111]. This mechanistic explanation perfectly agrees with the decreasing activation temperature from $CsMgCl_3$ to $CsMgI_3$ required for an increase in the luminescence intensity of the Eu^{2+}-based $4f^6 5d \rightarrow 4f^7$ emission. The presented results are particularly useful in applications as high-energy detecting materials, which strongly rely on an interaction of excitons or defects with an embedded activator. In that sense, these materials may provide useful insight into the mechanistic details of exciton-activator interaction of halides.

IV. CONCLUSIONS

In this paper, the optical properties of Eu^{2+}-localized and self-trapped excitons in the quasi-one-dimensional linear chain salts $CsMgX_3$ ($X = \mathrm{Cl}$, Br, I) are investigated. The calculated DOS of the halides highly suggest that the excitons that form in these compounds are very similar to the well-investigated STEs in simple binary alkali halides and can, hence, be described as excitons of the form $X_2^- + e$. The band structures justify this idea due to the low curvature of the highest halide-based p-like valence band, implying a high effective mass of the holes and, correspondingly, the high curvature of the lowest Mg-based s-like conduction band implying a low effective mass of the delocalized electron.

STE luminescence can be observed in the UV range in all three halides. The low Rabin-Klick parameters imposed by the densely packed crystal structure of the presented halides indicate a type I on-center (or $V_k + e$) configuration of the STEs. The decay times in the microsecond range of the excitonic transitions imply a triplet or π luminescence that is typical for STEs in halides. Both the emission energy and the increasing spin-orbit coupling play a role in the actual value of the decay time. In addition, IL STEs in Eu^{2+}-doped $CsMgX_3$ show intense

photoluminescence in the blue range at 10 K and can be readily identified by their excitation spectra, which are strikingly similar to the excitation spectra based on the $4f^7 \rightarrow 4f^6 5d$ transitions of the Eu^{2+}-doped halides $CsSrX_3$, respectively. Their intrinsic nature is also proven by doping with Sr^{2+} ions instead of Eu^{2+} ions. From the afterglow components of the decay curves of the IL STE–based emissions, a $t^{-0.4}$ to $t^{-0.7}$ dependence is found that additionally indicates a trapping of the excitons at the Eu^{2+} impurities.

Finally, the interaction of the excitons with local Eu^{2+} impurities is investigated by means of temperature-dependent luminescence studies. An energy transfer from the excitons to the local Eu^{2+} impurities is evident and can be interpreted in terms of thermal annihilation of the excitons. In this context, it is very remarkable that the luminescence intensity of the Eu^{2+}-based $4f^6 5d \rightarrow 4f^7$ emission in $CsMgBr_3:Eu^{2+}$ is much higher at room temperature than at low temperatures, which may be generally valid for an understanding of such observations. The activation energy for the energy transfer decreases from $CsMgCl_3$ to $CsMgI_3$, which is related to the decreasing bond strength of the self-trapped hole (X_2^-) for heavier halides. This study provides valuable insights into the mechanistic details of the nonradiative interaction between excitons and activators that may have relevance for the optimization of high-energy detecting materials such as scintillators or storage phosphors.

[1] W. M. Yen, S. Shionoya, and H. Yamamoto, *Phosphor Handbook*, 2nd ed. (CRC Press, Boca Raton, 2007).

[2] P. A. Rodnyi, *Physical Processes in Inorganic Scintillators* (CRC Press, Boca Raton, 1997).

[3] P. Lecoq, A. Annenkov, A. Gektin, M. Korzhik, and C. Pedrini, *Inorganic Scintillators for Detector Systems* (Springer, Heidelberg, 2006).

[4] H. H. Rüter, H. v. Seggern, R. Reininger, and V. Saile, Creation of Photostimulable Centers in $BaFBr:Eu^{2+}$ Single Crystals by Vacuum-Ultraviolet Radiation, Phys. Rev. Lett. **65**, 2438 (1990).

[5] M. Thoms, H. v. Seggern, and A. Winnacker, Spatial correlation and photostimulability of defect centers in the x-ray-storage phosphor $BaFBr:Eu^{2+}$, Phys. Rev. B **44**, 9240 (1991).

[6] H. Fröhlich, H. Pelzer, and S. Zienau, Properties of slow electrons in polar materials, Lond. Edinb. Dubl. Phil. Mag. J. Sci. **41**, 221 (1950).

[7] H. Fröhlich, Electrons in lattice fields, Adv. Phys. **3**, 325 (1954).

[8] Y. Toyozawa, Theory of the electronic polaron and ionization of a trapped electron by an exciton, Prog. Theor. Phys. **12**, 421 (1954).

[9] H. Haken and W. Schottky, Die Behandlung des Exzitons nach der Vielteilchentheorie, Z. Phys. Chem. (Frankfort/Main) **16**, 218 (1958).

[10] M. N. Kabler, Low-temperature recombination luminescence in alkali halide crystals, Phys. Rev. **136**, A1296 (1964).

[11] R. B. Murray and F. J. Keller, Recombination luminescence from V_K centers in potassium iodide, Phys. Rev. **137**, A942 (1965).

[12] R. B. Murray and F. J. Keller, V_K centers and recombination luminescence in rubidium iodide and sodium iodide, Phys. Rev. **153**, 993 (1967).

[13] D. Pooley and W. A. Runciman, Recombination luminescence in alkali halides, J. Phys. C **3**, 1815 (1970).

[14] R. S. Knox and N. Inchauspé, Exciton states in ionic crystals, Phys. Rev. **116**, 1093 (1959).

[15] M. N. Kabler and D. A. Patterson, Evidence for a Triplet State of the Self-Trapped Exciton in Alkali-Halide Crystals, Phys. Rev. Lett. **19**, 652 (1967).

[16] T. G. Castner and W. Känzig, The electronic structure of V-centers, J. Phys. Chem. Solids **3**, 178 (1957).

[17] W. B. Fowler, M. J. Marrone, and M. N. Kabler, Theory of self-trapped exciton luminescence in halide crystals, Phys. Rev. B **8**, 5909 (1973).

[18] M. J. Marrone, F. W. Patten, and M. N. Kabler, EPR in Triplet States of the Self-Trapped Exciton, Phys. Rev. Lett. **31**, 467 (1973).

[19] A. Wasiela, G. Ascarelli, and Y. Merle d'Aubigné, Optical Detection of Paramagnetic Resonance of the Self-Trapped Exciton in KBr, Phys. Rev. Lett. **31**, 993 (1973).

[20] R. T. Williams and K. S. Song, The self-trapped exciton, J. Phys. Chem. Solids **51**, 679 (1990).

[21] K. S. Song and R. T. Williams, *Self-Trapped Excitons*, 2nd ed. (Springer, Berlin, 1995).

[22] T. L. Gilbert and A. C. Wahl, Single-configuration wavefunctions and potential curves for low-lying states of He_2^+, Ne_2^+, Ar_2^+, F_2^-, Cl_2^- and the ground state of Cl_2, J. Chem. Phys. **55**, 5247 (1971).

[23] P. W. Tasker, G. G. Balint-Kurti, and R. N. Dixon, A calculation of the potential curves for the halogen molecule negative ions, Mol. Phys. **32**, 1651 (1976).

[24] H. N. Hersh, Proposed excitonic mechanism of color-center formation in alkali halides, Phys. Rev. **148**, 928 (1966).

[25] G. Brunet, C. H. Leung, and K. S. Song, Off-center configuration of the self-trapped exciton in potassium halides, Solid State Commun. **53**, 607 (1985).

[26] K. S. Song and C. H. Leung, A theoretical study of the π-luminescence from self-trapped excitons in alkali halide crystals, J. Phys. Condens. Matter **1**, 8425 (1989).

[27] Y. Toyozawa, A proposed model of excitonic mechanism for defect formation in alkali halides, J. Phys. Soc. Jpn. **44**, 482 (1978).

[28] K. Kan'no, T. Matsumoto, and T. Hayashi, New aspects of intrinsic luminescence in alkali halides, Rev. Solid State Sci. **4**, 383 (1990).

[29] K. Kan'no, T. Matsumoto, and Y. Kayanuma, Parity-broken and -unbroken self-trapped excitons in alkali halides, Pure Appl. Chem. **69**, 1227 (1997).

[30] W. Meise, U. Rogulis, F. W. Koschnick, K. S. Song, and J. M. Spaeth, Experimental evidence for spatial correlation between F and H centres formed by exciton decay at low temperatures in KBr, J. Phys. Condens. Matter **6**, 1815 (1994).

[31] H. Rabin and C. C. Klick, Formation of *F* centers at low and room temperatures, Phys. Rev. **117**, 1005 (1960).

[32] P. D. Townsend, A new interpretation of the Rabin and Klick diagram, J. Phys. C **6**, 961 (1973).

[33] M. Yuste, L. Taurel, and M. Rahmani, ESR and optical study of $[Cl_2^-]$ centre in BaClF crystal, Solid State Commun. **17**, 1435 (1975).

[34] M. Yuste, L. Taurel, M. Rahmani, and D. Lemoyne, Optical absorption and ESR study of F centres in BaClF and SrClF crystals, J. Phys. Chem. Solids **37**, 961 (1976).

[35] R. C. Baetzold, Atomistic simulation of defects in alkaline-earth fluorohalide crystals, Phys. Rev. B **36**, 9182 (1987).

[36] A. Ohnishi, K. Kan'no, Y. Iwabuchi, and N. Mori, Recombination luminescence from self-trapped excitons in BaFBr, Nucl. Instrum. Methods Phys. Res., Sect. B **91**, 210 (1994).

[37] M. Itoh, Studies of self-trapped exciton luminescence in ammonium halides, J. Phys. Soc. Jpn. **57**, 372 (1988).

[38] M. Itoh, Coexistence of free and self-trapped excitions in NH_4I, J. Phys. Soc. Jpn. **58**, 2994 (1989).

[39] R. Alcala, N. Koumvakalis, and W. A. Sibley, The self-trapped hole and thermoluminescence in $KMgF_3$, Phys. Status Solidi (a) **30**, 449 (1975).

[40] J. T. Lewis, J. L. Kolopus, E. Sonder, and M. M. Abraham, Reorientation and motion of the self-trapped hole in $KMgF_3$, Phys. Rev. B **7**, 810 (1973).

[41] N. Koumvakalis and W. A. Sibley, Radiation damage of $RbMgF_3$, Phys. Rev. B **13**, 4509 (1976).

[42] A. S. Voloshinovskii, V. B. Mikhailik, and P. A. Rodnyi, Luminescence of on- and off-center STE in ABX_3 crystals, Radiat. Eff. Defects Solids **135**, 281 (1995).

[43] J. Goodyear and D. J. Kennedy, The crystal structure of $CsMnBr_3$, Acta Crystallogr. Sect. B **28**, 1640 (1972).

[44] C. K. Møller, About the crystal structure of cesium cadmium tribromide, and some observations on crystals of cesium cadmium trichloride, Acta Chem. Scand. **31a**, 669 (1977).

[45] G. L. McPherson, A. M. McPherson, and J. L. Atwood, Structures of $CsMgBr_3$, $CsCdBr_3$ and $CsMgI_3$–Diamagnetic linear chain lattices, J. Phys. Chem. Solids **41**, 495 (1980).

[46] C. Andraud, F. Pellé, O. Pilla, J. P. Denis, and B. Blanzat, Self-localized excitons in cesium tribromocadmate, Cryst. Lattice Defects Amorphous Mater. **16**, 395 (1987).

[47] C. Andraud, F. Pellé, O. Pilla, and B. Blanzat, Intrinsic luminescence of $CsCdBr_3$, Phys. Status Solidi (b) **149**, 759 (1988).

[48] M. Wenzel, M. Altwein, R. Demirbilek, B. Leu, J. Heber, J. Kübler, B. Bleeker, and A. Meijerink, Band structure and excitons in $CsCdBr_3$, J. Alloys Compd. **300–301**, 479 (2000).

[49] J. Heber, R. Demirbilek, M. Altwein, J. Kübler, B. Bleeker, and A. Meijerink, Electronic states and interactions in pure and rare-earth doped $CsCdBr_3$, Radiat. Eff. Defects Solids **154**, 223 (2001).

[50] J. Heber, R. Demirbilek, and S. I. Nikitin, Excitons and rare-earth ions in $CsCdBr_3$, J. Alloys Compd. **380**, 50 (2004).

[51] S. García-Revilla and R. Valiente, *f*-*d* transitions and self-trapped excitons in $CsCdBr_3:Eu^{2+}$, J. Phys. Condens. Matter **18**, 11139 (2006).

[52] K. F. Talluto, V. F. Trautmann, and G. L. McPherson, Energy transfer in linear chain manganese salts: Emission spectra of $CsMnBr_3$, $RbMnBr_3$ and $CsMnI_3$ crystals doped with Er^{3+}, Chem. Phys. **88**, 299 (1984).

[53] W. J. Rodriguez, R. Auerbach, and G. L. McPherson, Exciton annihilation in photoexcited crystals containing divalent manganese, Chem. Phys. Lett. **132**, 558 (1986).

[54] Y. Toyozawa and Y. Shinozuka, Stability of an electron in deformable lattice–Force range, dimensionality and potential barrier, J. Phys. Soc. Jpn. **48**, 472 (1980).

[55] S. L. Dexheimer, A. D. V. Pelt, J. A. Brozik, and B. I. Swanson, Femtosecond Vibrational Dynamics of Self-Trapping in a Quasi-One-Dimensional System, Phys. Rev. Lett. **84**, 4425 (2000).

[56] F. X. Morrisey, J. G. Mance, A. D. V. Pelt, and S. L. Dexheimer, Femtosecond dynamics of exciton localization: Self-trapping from the small to the large polaron limit, J. Phys. Condens. Matter **25**, 144204 (2013).

[57] O. T. Antonyak, A. S. Voloshinovskii, I. P. Pashuk, S. N. Pidzyrailo, and P. A. Rodnyi, Intrinsic luminescence of cesium magnesium chloride ($CsMgCl_3$) crystals, Opt. Spektrosk. **70**, 1035 (1991).

[58] A. P. Shpak, O. A. Glike, A. G. Dmitriev, P. A. Rodnyi, A. S. Voloshinovskii, and S. M. Pidzyrailo, Radiative core-valence transitions in wide-gap crystals, J. Electron Spectrosc. Relat. Phenom. **68**, 335 (1994).

[59] M. A. Macdonald, E. N. Mel'chakov, I. H. Munro, P. A. Rodnyi, and A. S. Voloshinovskii, Radiative core-valence transitions in $CsMgCl_3$ and $CsSrCl_3$, J. Lumin. **65**, 19 (1995).

[60] J. K. Howell and L. L. Pytlewski, Synthesis of divalent europium and ytterbium halides in liquid ammonia, J. Less-Common Met. **18**, 437 (1969).

[61] W. Klemm and W. Döll, Messungen an zwei- und vierwertigen Verbindungen der seltenen Erden. VI. Zur Kenntnis der Halogenide des zweiwertigen Europiums, Z. Anorg. Allg. Chem. **241**, 233 (1939).

[62] M. D. Taylor and C. P. Carter, Preparation of anhydrous lanthanide halides, especially iodides, J. Inorg. Nucl. Chem. **24**, 387 (1962).

[63] J. M. Haschke and H. A. Eick, The preparation and some properties of europium bromides and hydrated bromides, J. Inorg. Nucl. Chem. **32**, 2153 (1970).

[64] G. Meyer, S. Dötsch, and T. Staffel, The ammonium-bromide route to anhydrous rare earth bromides MBr_3, J. Less-Common Met. **127**, 155 (1987).

[65] V. L. Cherginets, A. Y. Grippa, T. P. Rebrova, Y. N. Datsko, T. V. Ponomarenko, N. V. Rebrova, N. N. Kosinov, O. A. Tarasenko, Y. I. Dolzhenko, and O. V. Zelenskaya, Scintillation properties of Eu^{2+}-doped $SrCl_2$ and $CsSrCl_3$ single crystals, Funct. Mater. **19**, 187 (2012).

[66] M. Suta, P. Larsen, F. Lavoie-Cardinal, and C. Wickleder, Photoluminescence of $CsMBr_3:Eu^{2+}(M = Mg, Ca, Sr)$–A novel strategy for the development of low-energy emitting phosphors, J. Lumin. **149**, 35 (2014).

[67] M. Suta and C. Wickleder, Photoluminescence of $CsMI_3:Eu^{2+}$ (M = Mg, Ca, and Sr)–A spectroscopic probe on structural distortions, J. Mater. Chem. C **3**, 5233 (2015).

[68] B. E. Markov and I. D. Panchenko, Composition diagrams for the binary systems of magnesium chloride with the

chlorides of the alkali metals, Zh. Obshch. Khim. **25**, 2042 (1955).
[69] H. H. Emons, G. Bräutigam, and W. Horlbeck, Untersuchungen zum Phasengleichgewicht fest-flüssig in binären Mischungen aus Erdalkalimetall- und Alkalimetallbromiden, Chem. Zvesti **30**, 748 (1976).
[70] H. J. Seifert, B. Müller, and E. Stötzel, Thermochemische und strukturelle Untersuchungen an Systemen aus Alkalimetallhalogenid und MgI_2 bzw. CaI_2, Rev. Chim. Miner. **17**, 147 (1980).
[71] See Supplemental Material at http://link.aps.org/supplemental/10.1103/PhysRevApplied.9.064024 for x-ray powder diffraction patterns of the undoped halides $CsMgX_3$ ($X = Cl, Br, I$) and photoluminescence excitation spectra of undoped $CsMgBr_3$ and $CsMgBr_3:1\%\,Sr^{2+}$ for comparison.
[72] J. Hafner, G. Kresse, D. Vogtenhuber, M. Marsman, and J. Furthmüller, Vienna *ab initio* simulation package, Computational Materials Physics, Vienna, 2014 [http://www.vasp.at/].
[73] G. Kresse and J. Hafner, *Ab initio* molecular dynamics for liquid metals, Phys. Rev. B **47**, 558 (1993).
[74] G. Kresse and J. Hafner, *Ab initio* molecular-dynamics simulation of the liquid-metal-amorphous-semiconductor transition in germanium, Phys. Rev. B **49**, 14251 (1994).
[75] G. Kresse and J. Furthmüller, Efficiency of *ab-initio* total energy calculations for metals and semiconductors using a plane-wave basis set, Comput. Mater. Sci. **6**, 15 (1996).
[76] G. Kresse and J. Furthmüller, Efficient iterative schemes for *ab initio* total-energy calculations using a plane-wave basis set, Phys. Rev. B **54**, 11169 (1996).
[77] J. P. Perdew and Y. Wang, Accurate and simple analytic representation of the electron-gas correlation energy, Phys. Rev. B **45**, 13244 (1992).
[78] J. P. Perdew, J. A. Chevary, S. H. Vosko, K. A. Jackson, M. R. Pederson, D. J. Singh, and C. Fiolhais, Atoms, molecules, solids, and surfaces: Applications of the generalized gradient approximation for exchange and correlation, Phys. Rev. B **46**, 6671 (1992).
[79] J. P. Perdew, J. A. Chevary, S. H. Vosko, K. A. Jackson, M. R. Pederson, D. J. Singh, and C. Fiolhais, Atoms, molecules, solids, and surfaces: Applications of the generalized gradient approximation for exchange and correlation, Phys. Rev. B **48**, 4978 (1993).
[80] P. E. Blöchl, Projector augmented-wave method, Phys. Rev. B **50**, 17953 (1994).
[81] G. Kresse and D. Joubert, From ultrasoft pseudopotentials to the projector augmented-wave method, Phys. Rev. B **59**, 1758 (1999).
[82] G. McPherson and K. Talluto, Luminescent centers in doped crystals of $CsMgI_3$: Energy storage and thermoluminescence, Solid State Commun. **43**, 331 (1982).
[83] G. L. McPherson, T. J. Kistenmacher, and G. D. Stucky, Single-crystal paramagnetic resonance studies of V(II), Mn(II), and Ni(II) in $CsMgCl_3$ and the crystal structure of $CsMgCl_3$, J. Chem. Phys. **52**, 815 (1970).
[84] G. Shwetha, V. Kanchana, and G. Vaitheeswaran, $CsMgCl_3$: A promising cross luminescence material, J. Solid State Chem. **227**, 110 (2015).
[85] R. W. Godby, M. Schlüter, and L. J. Sham, Trends in self-energy operators and their corresponding exchange-correlation potentials, Phys. Rev. B **36**, 6497 (1987).
[86] R. O. Jones and O. Gunnarsson, The density functional formalism, its applications and prospects, Rev. Mod. Phys. **61**, 689 (1989).
[87] J. P. Perdew, R. G. Parr, M. Levy, and J. L. Balduz, Jr., Density-Functional Theory for Fractional Particle Number: Derivative Discontinuities of the Energy, Phys. Rev. Lett. **49**, 1691 (1982).
[88] P. Mori-Sánchez and A. J. Cohen, The derivative discontinuity of the exchange-correlation functional, Phys. Chem. Chem. Phys. **16**, 14378 (2014).
[89] G. L. McPherson, Y. Y. Waguespack, T. C. Vanoy, and W. J. Rodriguez, Exciton migration in a "pseudo"-one-dimensional crystal: Luminescence dynamics of doped $CsMnBr_3$, J. Chem. Phys. **92**, 1768 (1990).
[90] R. L. Blakley, C. E. Martinez, M. F. Herman, and G. L. McPherson, Exciton annihilation in one-dimensional inorganic crystals: power dependent luminescence decay curves from $(CH_3)_4NMnCl_3$ (TMMC), $(CH_3)_4NMnBr_3$ (TMMB) and $CsMnBr_3$ (CMB), Chem. Phys. **146**, 373 (1990).
[91] L. S. Xiao, M. Lang, and P. S. May, Optical properties of Eu-doped and Eu-Gd Co-doped $CsMgCl_3$: temperature dependence of rate constants for $^5D_2$ and $^5D_1$ cross relaxation in symmetric Eu(III)-Eu(III) pairs, J. Phys. Chem. A **104**, 209 (2000).
[92] H. Ramanantoanina, F. Cimpoesu, C. Göttel, M. Sahnoun, B. Herden, M. Suta, C. Wickleder, W. Urland, and C. Daul, Prospecting lighting applications with ligand field tools and density functional theory: A first-principles account of the $4f^7$-$4f^6 5d^1$ luminescence of $CsMgBr_3:Eu^{2+}$, Inorg. Chem. **54**, 8319 (2015).
[93] J. H. Radhakrishnan and S. Selvasekarapandian, Photoluminescence of undoped and Eu doped CsCl crystals, J. Phys. Condens. Matter **6**, 6035 (1994).
[94] P. Hackenschmied, G. Zeitler, M. Batentschuk, A. Winnacker, B. Schmitt, M. Fuchs, E. Hell, and W. Knüpfer, Storage performance of x-ray irradiated doped CsBr, Nucl. Instrum. Methods Phys. Res., Sect. B **191**, 163 (2002).
[95] H. J. Seo, W. S. Zhang, T. Tsuboi, S. H. Doh, W. G. Lee, H. D. Kang, and K. W. Jang, Luminescence properties of a CsI crystal doped with Eu^{2+} ions, J. Alloys Compd. **344**, 268 (2002).
[96] R. D. Shannon, Revised effective ionic radii and systematic studies of interatomic distances in halides and chalcogenides, Acta Cryst. **A32**, 751 (1976).
[97] P. Dorenbos, Anomalous luminescence of Eu^{2+} and Yb^{2+} in inorganic compounds, J. Phys. Condens. Matter **15**, 2645 (2003).
[98] P. S. Senanayake, J.-P. R. Wells, M. F. Reid, G. Berden, A. Meijerink, and R. J. Reeves, Electron trap liberation in MgF_2 doped with Yb^{2+} using a two-color excitation experiment, Appl. Phys. Lett. **100**, 041902 (2012).
[99] P. S. Senanayake, J.-P. R. Wells, M. F. Reid, G. Berden, A. Meijerink, and R. J. Reeves, Impurity-trapped excitons and electron traps in $CaF_2:Yb^{2+}$ and $SrF_2:Yb^{2+}$ probed by transient photoluminescence enhancement, J. Lumin. **133**, 81 (2013).

[100] Z. Barandiarán and L. Seijo, Intervalence charge transfer luminescence: Interplay between anomalous and $5d$-$4f$ emissions in Yb-doped fluorite-type crystals, J. Chem. Phys. **141**, 234704 (2014).

[101] R. B. Hughes-Currie, P. S. Senanayake, J.-P. R. Wells, M. F. Reid, G. Berden, R. J. Reeves, and A. Meijerink, Site-selective transient photoluminescence enhancement of impurity-trapped excitons in $NaMgF_3:Yb^{2+}$, Phys. Rev. B **88**, 104304 (2013).

[102] P. S. Senanayake, J.-P. R. Wells, M. F. Reid, R. B. Hughes-Currie, G. Berden, R. J. Reeves, and A. Meijerink, Frequency non-degenerate sequential excitation of the impurity trapped exciton in strontium fluoride crystals doped with ytterbium, J. Appl. Phys. **117**, 133109 (2015).

[103] R. B. Hughes-Currie, A. J. Salkeld, K. V. Ivanovskikh, M. F. Reid, J.-P. R. Wells, and R. J. Reeves, Excitons and interconfigurational transitions in $CaF_2:Yb^{2+}$ crystals, J. Lumin. **158**, 197 (2015).

[104] R. B. Hughes-Currie, K. V. Ivanovskikh, M. F. Reid, J.-P. R. Wells, R. J. Reeves, and A. Meijerink, Vacuum ultraviolet synchrotron measurements of excitons in $NaMgF_3:Yb^{2+}$, J. Lumin. **169**, 419 (2016).

[105] H. Nakagawa and M. Kitaura, Non-radiative branching processes of self-trapped excitons in cadmium halide crystals, Proc. SPIE Int. Soc. Opt. Eng. **2362**, 294 (1995).

[106] J. Heber, J. Neukum, M. Altwein, R. Demirbilek, and N. Bodenschatz, Interaction between excitons and rare-earth ions, Spectrochim. Acta, Part A **54**, 1557 (1998).

[107] R. D. Wieting, M. D. Fayer, and D. D. Dlott, The effects of impurity scattering and transport topology on trapping in quasi-one-dimensional systems: Application to excitons in molecular crystals, J. Chem. Phys. **69**, 1996 (1978).

[108] T. Förster, Zwischenmolekulare Energiewanderung und Fluoreszenz, Ann. Phys. (Berlin) **437**, 55 (1948).

[109] D. L. Dexter, A theory of sensitized luminescence in solids, J. Chem. Phys. **21**, 836 (1953).

[110] M. Krings, G. Montana, R. Dronskowski, and C. Wickleder, α-$SrNCN:Eu^{2+}$–A novel efficient orange-emitting phosphor, Chem. Mater. **23**, 1694 (2011).

[111] J. G. Dojahn, E. C. M. Chen, and W. E. Wentworth, Characterization of homonuclear diatomic ions by semi-empirical Morse potential energy curves. 1. The halogen anions, J. Phys. Chem. **100**, 9649 (1996).